Supporting Information

Isojima et al. 10.1073/pnas.0908733106

SI Text

Detailed Procedures of the Screenings of Chemical Compounds That Affect the Period Length Both in Mouse and Human Clock Cells. As described in the main text, we examined 1,260 pharmacologically active chemical compounds from the LOPAC^{1280} library (Sigma-Aldrich) (1). We first screened this library with relatively high concentrations (25 μM for NIH 3T3-*mPer2-Luc* and 50 μM for U2OS-*hPer2-Luc*) to reduce false negatives. We found 253 compounds for NIH 3T3-*mPer2-Luc* cells and 294 compounds for U2OS-*hPer2-Luc* cells that either altered the period length by more than 3 s.d. from the negative control or induced apparent arrhythmicity. The intersection of these data yielded 166 compounds: Six and 40 compounds that shortened and lengthened, respectively, the period length of both cell types, and 120 compounds that induced apparent arrhythmicity (including compounds that were potentially cytotoxic or could affect the LUC readout) in both cell types (Table S1).

To confirm the efficacy of the 166 compounds selected above, and to exclude potentially cytotoxic or LUC-readout altering compounds, we conducted dose-dependency assays using the two clock cell lines. Three concentrations of each compound were tested for period-altering effects of approximately one order of magnitude from the concentration used in the primary assay (25, 8.3, and 2.8 μM for NIH 3T3-*mPer2-Luc*; and 50, 16.7, and 5.6 μM for U2OS-*hPer2-Luc*). If the lowest concentration of a compound induced an apparent arrhythmicity in the cells, two additional decreases in concentration were tested (0.93 and 0.31 μM for NIH 3T3-*mPer2-Luc*; 1.9 and 0.62 μM for U2OS-*hPer2-Luc*). This experiment identified nine compounds that significantly shortened ($<$-3 s.d.) and 30 that significantly lengthened ($>$+3 s.d.) the period length of NIH 3T3-*mPer2-Luc* cells, and seven and 90 compounds that shortened and lengthened, respectively, the period length of U2OS-*hPer2-Luc* cells (Table S2). After integrating these data across the cell types, we found four and 24 compounds that respectively shortened and lengthened the period of both cell lines. We designated these 28 compounds as "effective" compounds, and we believe they will be a useful chemical resource for circadian biology (Table S3 and Table S4). We further examined these compounds to find those with the "potent" effects ($>$+10 s.d. or $<$-10 s.d., ≈2.0–3.0 h) as described in the main text.

Chemical Landscape of Period Determination in Mammalian Circadian Clocks. As described in the main text, a chemical-biological approach was recently proposed to help elucidate the basic processes underlying circadian clocks (2). Working on a relatively small scale, previous studies revealed that several protein kinase inhibitors [such as IC261 (3, 4), CKI-7 (5), lithium chloride (6, 7), SP600125 (4, 8), and SB203580 (9)], adenylate cyclase inhibitors [such as THFA (9-tetrahydro-2-furyl-denine), 2′5′-dideoxyadonosine, and 9-cyclopentyladenine (4)], and proteasome inhibitors [such as MG132 and lactacystin (3)], can lengthen the period of mammalian circadian clocks by 2% to ≈40%. Moreover, high-throughput screening of a large chemical compound library (1) supported using a chemical-biological approach to probe the fundamental processes of the mammalian circadian clock.

This study presents a chemical-biological approach to controlling, analyzing, and exploring the period-determination processes in the mammalian circadian clock. Using this approach, we identified 28 chemical compounds that significantly ($>$3 s.d.) altered the period length of both human and mouse clock cell lines (Table S3 and Table S4). Among them, 10 "potent" compounds markedly ($>$10 s.d.) lengthened the period (Fig. S1 *A* and *D*), and lengthened it in both peripheral clock cells (MEFs) and central clock tissues (SCN) (Fig. S1 *B*, *C*, and *E*). These results suggest that our protocol, which featured a high-throughput chemical screening strategy and multiple cell lines of different origin [NIH 3T3 and U2OS cells were derived from NIH/Swiss mouse embryo cultures (10) and from human osteocarcinoma cells (11), respectively], and which applied a stringent threshold for "potency," enabled the identification of exceptionally potent chemical probes that target fundamental processes in mammalian circadian clocks. By probing this "chemical landscape," we uncovered "potent," "effective," and even "ineffective" compounds, which will serve as a useful guide for drug researchers seeking cures for rhythm disorders.

So far, this chemical landscape features at least two salient landmarks: One is the period-determining process targeted by 17-OHP and the other is the period-determining process targeted by CKIε/δ activity. Since progesterone and progestins, synthetic progesterone derivatives such as 17-hydroxyprogesterone caproate and medroxyprogesterone, are widely available as clinical drugs (12), the 17-OHP "landmark" serves as a good vantage point for putative therapeutics (Fig. S1) to mitigate rhythm disorders such as advanced sleep phase syndrome (ASPS) (i.e., via an agonist like 17-OHP). While guiding drug discovery, the landmarks on this revealing chemical landscape will also be useful for further exploration of the fundamental properties of mammalian circadian clocks.

Validity of Relatively Higher-Dose Applications of Potent Effective Compounds in Vitro and in Cellulo. In this chemical-biological study, we discovered a highly flexible period-lengthening response in the mammalian clock: A human clock cell's circadian period could be stretched into a circabidian period (Fig. 2*A*) through chemical manipulation, probably of the CKI activity, by SP600125 and TG003. The half-maximum concentrations of these compounds for their period-lengthening effect in cellulo were ≈22 and 63 μM, respectively. In contrast, the IC_{50}s of SP600125 and TG003 for the CKIε kinase activity with 20 μM ATP in vitro were ≈0.22 and 0.55 μM, respectively (Fig. 1*E*). If these compounds function as competitive inhibitors for ATP, this apparent discrepancy can be largely explained by the difference in ATP concentration, which is ≈1 mM inside cells (13–15). This competitive-inhibition hypothesis is experimentally supported by our observations that higher amounts of inhibitors were required in assays with a high concentration of ATP (100 μM ATP; Fig. 1*D*) than with a lower concentration (20 μM ATP; Fig. 1E). Given that the Michaelis constant for ATP with CKIε is ≈20 μM, the ratio of the IC_{50} with 1 mM ATP (in cellulo) to that with 20 μM ATP (in vitro kinase assay) is 25.5, and hence the IC_{50}s of SP600125 and TG003 with 1 mM ATP should be ≈5.6 and 14.5 μM, respectively. Although there is still a 4-fold difference between the half-maximum concentrations in cellulo and the estimated IC_{50}s with 1 mM ATP, these values are within the same order of magnitude. The difference might be owing to the dynamics of these compounds in cellulo, such as the efficiency of their penetration into cells, nonspecific buffering by other proteins within cells, and excretion from cells. Another possibility is that these potent compounds act on other targets in addition to CKIε and CKIδ, such as their "primary" targets, which might be strongly involved in the period-determining processes of mammalian circadian clocks. However, the latter

possibility was not supported by the results of our siRNA experiments, in which we knocked down kinases including the "primary" targets of the potent compounds (Fig. S2).

Temperature-Insensitivity of CKI Phosphorylation Depended on the Substrate Recognition. CKIs recognize the motif "Ser/Thr-x-x-Ser/Thr," and phosphorylate the Ser/Thr residue at the C-terminal end. Negative charge at the N-terminal end of the motif was thought to be the "priming signal" of the CKI-dependent phosphorylation, because phosphorylation of the Ser/Thr residue at the N-terminal end or replacement of the residue to the acidic amino acid (Glu or Asp) remarkably improved the efficiency of the CKI-dependent phosphorylation (16). As described in the main text, phosphorylation of βTrCP peptide or FASPS-peptide by ΔCKIε(wt) were relatively temperature-insensitive (βTrCP; Q_{10} = 1.0, FASPS; Q_{10} = 1.2), although that of CK1tide was more temperature-sensitive (CK1tide; Q_{10} = 1.4) (Fig. 3). It should be noted that the CK1tide was "primed," but the former two substrates were not. Moreover, the *tau* mutation (R178C) of CKIε, which are thought to affect substrate recognition of CKIε, resulted to become temperature-sensitive in the phosphoryaltion of the FASPS-peptide (Q_{10} = 1.6). These results implied that substrate recognition by CKIε/δ was a crucial process for defining temperature-dependency of CKIε/δ-dependent phosphorylation. We also noted that priming phosphorylation at a Ser-662 residue of hPER2, associating with FASPS, was regulating protein stability and nuclear translocation or transcriptional repressor activity, although a kinase responsible for the priming phosphorylation have not been identified (17).

SI Materials and Methods

Establishment of a High-Throughput Screening System Using a Cooled CCD-Camera (CCD-Tron System). To perform high-throughput screening of a chemical compound library, we developed a screening system that uses a high-performance CCD camera, based on a monitoring system using photomultiplier tubes (PMT) described in a previous report (PMT-Tron system) (18). The round turntable (Mashinax or NEXSYS Corp.) enables the observation of up to 12 culture plates at once, and thus 4,608 samples can be screened simultaneously if 384-well culture plates are used. The computer-controlled turntable rotates and sequentially sets each of the plates under the CCD camera every 5 min. The bioluminescence from the culture plate is imaged by the high-performance CCD camera (VersArray XP or PIXIS; Roper Scientific). The intensity of each well is calculated from the obtained image by a custom-made computer program

Establishment of Stable Transfectants of NIH 3T3 Cells Expressing the *mPer2-Luc* Reporter. The mouse *Per2* promoter-driven reporter plasmid (*mPer2-Luc*) (19) and the pIREShyg3 plasmid (BD Biosciences) were cotransfected into NIH 3T3 cells with FuGene6 transfection reagent (Roche). NIH 3T3 clones expressing *mPer2-Luc* (NIH 3T3-*mPer2-Luc*) were selected using 200 μg/mL hygromycin B (Invitrogen).

Establishment of Stable Transfectants of U2OS Cells Expressing the *hPer2-Luc* Reporter. A 334-bp fragment of the human *Per2* gene promoter, 502- to 169-bp upstream from exon 1, was amplified by PCR with PrimeSTAR DNA polymerase (TaKaRa) and the following primers:

F: 5′-GGGGTACCGAGGGCGTAGTGAATGGAAG-3′
R: 5′-CCCAAGCTTAGCTGCACGTATCCCCTCAG-3′

This promoter fragment was subcloned into the reporter vector, pGL4.14 (Promega) with the restriction enzymes, *Kpn*I and *Hin*dIII (TaKaRa). This *hPer2* promoter-driven reporter plasmid (*hPer2-Luc*) was transfected into U2OS cells (purchased from American Type of Culture Collections; ATCC), and stable transfectants (U2OS-*hPer2-Luc*) were selected as described for the NIH 3T3 cells.

Preparation of Embryonic Fibroblasts from *mPer2^{Luc}* Mice. The *mPer2^{Luc}* mice (20) were carefully kept and handled according to the RIKEN Regulations for Animal Experiments. Embryos of *mPer2^{Luc}* mice at E13 ≈15 were excised and washed several times with Hanks' balanced salt solution. After the placenta and internal organs were completely removed, the embryos were cut into small pieces, and the cells were dissociated by incubation in 0.05% trypsin solution with 0.53 mM EDTA for 30 min at 37 °C. The dissociated cells (mouse embryonic fibroblasts from *mPer2^{Luc}* mice; *mPer2^{Luc}* MEFs) were suspended and cultured in the growth medium (DMEM supplemented with 10% FBS).

Preparation of SCN Slices from *mPer2^{Luc}* Mice. The brains were removed from quickly decapitated, young (older than 4 weeks of age) *mPer2^{Luc}* mice, then 300-μm-thick coronal sections containing the SCN were made using a vibratome type linearslicer (PRO7; Dosaka EM Corp) in ice cold Hanks' balanced salt solution (Invitrogen). The slices were then placed on a culture membrane (MilliCell-CM; Millipore) and set on a dish with 1.2 mL culture medium [DMEM supplemented with 1.2 g/L $NaHCO_3$ (Nacalai Tesque), 15 mM HEPES (Dojindo), 20 mg/L kanamycin (Invitrogen), 5 μg/mL insulin (Sigma), 20 nM putrescine (Sigma), 100 μg/mL apo-transferrin (Sigma), 20 nM progesterone (Sigma), 30 nM sodium selenite (Sigma), one-fiftieth part B-27 supplement (Invitrogen), and 100 μM luciferin] containing the chemical compounds at the concentrations indicated in Fig. S1*C*.

Analysis of the Effects of Compounds on Period Length in Cultured Cells and Slices. NIH 3T3-*mPer2-Luc* cells, U2OS-*hPer2-Luc* cells, and *mPe2^{Luc}* MEFs were cultured on 24-well (PerkinElmer), 96-well, or 384-well (Falcon) culture plates, and 300 μm-thick coronal slices containing the SCN from *mPe2^{Luc}* mice on a culture membrane (MilliCell-CM; Millipore) in medium supplemented with 200 μM luciferin (Promega) and a chemical compound with (cells) or without (slices) stimulation with 10 nM forskolin (Nacalai Tesque). The culture plates were placed in a high-sensitivity bioluminescence detection system (LM-2400; Hamamatsu Photonics, for slices; PMT-Tron for MEFs; or CCD-Tron, for others), and the bioluminescence of each well was measured at 30 °C (cells) or 37 °C (slices) (Fig. S1 *D* and *E*). The time-course bioluminescence data were analyzed as reported previously (18).

Rhythmicity and Period Length Analysis of Real-Time Bioluminescence Data. The rhythmicity and period length were determined from the bioluminescence data of NIH 3T3-*mPer2-Luc cells*, U2OS-*hPer2-Luc* cells, MEFs, and SCN slices, as previously reported (18). Although this method could not be used for samples with a period length longer than 36 h, we modified the analysis method to examine the long periods of circadian clocks in the presence of high concentrations of potent period-lengthening compounds (TG003 and SP600125) (Fig. 2*A*). The data obtained 36 h after the addition of forskolin and compound, instead of 21 h, were used for analysis to eliminate the first cycle, and detrending was performed not to detect the periodicity longer than 72 h, instead of 42 h in usual method. These modifications enabled us to examine periodicities up to 56 h.

Gene Knockdown Studies Using siRNA in U2OS-*hPer2-Luc* Cells. U2OS-*hPer2-Luc* cells were plated at 3.0×10^4 cells per well in 24-well multiwell plates, 24 h before the transfection. The predesigned *Silencer* Select siRNAs (Ambion) were transfected with Lipofectamine 2000 reagent (Invitrogen) as described in the manufacturer's protocol. At least three siRNA clones for each

gene were examined. The siRNA was used at 5 to 20 pmol/well, and the total amount of transfected siRNA was adjusted to 20 pmol/well using *Silencer* Select negative control #2 siRNA (Ambion).

A pair of culture plates was prepared for each transfection condition. The medium on one plate was changed to the recording medium containing 10 nM forskolin and 100 μM luciferin 24 h after the transfection, placed into the PMT-Tron system, and the period length was measured as described above. The total RNA of the cells on the other plate was purified with TRIzol reagent (Invitrogen), and the cDNA was reverse-transcribed using SuperScript II or III (Invitrogen) with random primers (Invitrogen), as described in the manufacturer's protocol. The gene expression levels were quantified with the QuantiFast SYBR PCR kit (Qiagen) with a LightCycler 480 (Roche Applied Science) or PRISM 7900 HT (PerkinElmer), according to the manufacturers' protocols.

The ID numbers of the predesigned *Silencer* Select siRNAs used in these studies were as follows:

Cry2. s3537; *CSNK1E*: s57, s58, and s59; *CSNK1D*: s3627, s3628, and s3629; *MAPK8*: s11152, s11153, and s11154; *MAPK9*: s11158, s11159, and s11160; *CLK1*: s3162, s3163, s3164; *CLK2*: s3165, s3166, and s3167; *CLK4*: s32986, s32987, and s32988; *CDK2*: s204, s205, and s206; *CDK5*: s2825, s2826, and s2827; *CDC2*: s463, s464, and s465: *MAPK14*: s3585, s3586, and s3587; *MAPK11*: s11155, s11156, and s11157; *MAPK12*: s12467, s12468, and s12469; *CSNK2A1*: s3636, s3637, and s3638; *CSNK2A2*: s3639, s3640, and s3641; *ADORA1*: s1085, s1086, and s1087; *ADORA2A*: s1088, s1089, and s1090; *ADORA2B*: s1091, s1092, and s1093. In addition, the following custom designed *Silencer* Select siRNAs were used:

CLK1: s229161 and s229162; *CLK2*: s229159 and s229160; *CLK4:* s229157 and s221958.

Expression and Purification of mCKIε/δ Protein. Mouse *CKIε* ORFs, corresponding to amino acids 2–416 (full-length CKIε) and 2–319 (ΔCKIε), and *CKIδ* ORFs, corresponding to amino acids 2–415 (full-length CKIδ) and 2–317 (ΔCKIδ), were cloned into the pGEX-6P-1 vector (GE Healthcare) and then introduced into *Escherichia coli* Rosetta2 (Novagen). A *CKIε* ORF in which eight serine residues identified as autophosphorylation amino acids (21) in the C-terminal region were replaced with glutamate, referred to as CKIε (D8), was also cloned and introduced into *E. coli*. Cells were grown at 25 °C until they reached an OD_{600} absorbance of about 0.5. After the addition of isopropyl β-D-1-thiogalactopyranoside (IPTG) to a final concentration of 0.1 mM, the cells were further grown at 25 °C for 24 h. The cells were collected and resuspended in extraction buffer [50 mM Tris-HCl, pH 7.5, 300 mM NaCl, 1 mM DTT, 1 mM EDTA, 10% glycerol, and complete protease inhibitor mixture (Roche)] and homogenized by sonication. The homogenate was spun at 38,000× *g*, and the supernatant was applied to a Glutathione Sepharose 4B column (GE Healthcare). The column was washed with five column volumes of the buffer. PreScission Protease (GE Healthcare) was then applied to the column to remove the GST-tag, according to the manufacturer's protocol. The proteins were eluted with two column volumes of elution buffer (50 mM Tris-HCl, pH 7.5, 300 mM NaCl, 1 mM DTT, 1 mM EDTA, and 10% glycerol), and the eluent was diluted and applied to a HiTrap SP HP column (GE Healthcare). The proteins were then eluted with 600 mM NaCl. The protein concentration was determined by the Bradford method, using the Bio-Rad Laboratories protein assay kit with BSA (Bio-Rad Laboratories) as a standard. The purified proteins used in this study are shown in Fig. S6 *B* and *C*.

Measurement of CKI Enzymatic Activity. ΔCKIε protein (0.5 μM) was added to the reaction buffer (25 mM Tris-HCl, pH 7.5, 7.5 mM $MgCl_2$, 1 mM DTT, 0.1 mg/mL BSA, and 200 nM synthetic peptide substrate) with different concentrations of chemicals (25, 50, or 100 μM for the potent compounds; 100 μM for IC261), preincubated at 30 °C for 5 min, and then the reaction was started by adding a one-fourth volume of 400 μM ATP. Aliquots (1 μL) of the reaction mixture were withdrawn in triplicate at 0 and 1 h of the reaction and mixed with 30 μL IMAP binding buffer in 384-well glass-bottomed plates (Olympus). After incubating for at least 1 h at ambient temperature, the fluorescent polarization was measured using a single-molecule fluorescence detection (SMFD) system (MF20; Olympus).

The measurement of CKI kinase activity using a P81 phosphocellulose paper assay was performed as follows. Peptides consisting of 34 aa (RKKKPHSGSSGYGSLGSNGSHEHLMSQTSSSDSN), referred to as βTrCP-peptide (22), and 29 aa (RKKKTEVSAHLSSLTLPGKAESVVSLTSQ), referred to as FASPS-peptide, were synthesized and purchased from Bio-Synthesis Inc. CK1tide (KRRRAL[pS]VASLPGL; Upstate), and α-casein from bovine milk (Sigma) were used as the substrate.

ΔCKIε/δ proteins (0.2 μM for βTrCP-peptide and FASPS-peptide, 0.02 μM for α-casein, 0.01 μM for CK1tide) in the reaction buffer (25 mM Tris, pH 7.5, 7.5 mM $MgCl_2$, 1 mM DTT, 0.1 mg/mL BSA, and 200 μM peptide substrate or 40 μM casein) were preincubated for 5 min. The reaction was started by adding a one-fourth volume of 2 mM (Fig. S6*D*), 400 μM (Fig. 1*D*), or 80 μM (Fig. 1*E*) ATP with 0.5–1 μCi [γ-^{32}P] ATP per reaction. In assays for autophosphorylated CKIε/δ (0.4 μM for βTrCP-peptide, 0.04 μM for α-casein, and CK1tide), the enzyme was preincubated with buffer (25 mM Tris, pH 7.5, 7.5 mM $MgCl_2$, 1 mM DTT, 0.1 mg/mL BSA, 500 μM ATP) at 30 °C for 1 h, and the reaction was started by adding substrate. The preincubation and incubation steps were performed at 25 ° or 35 °C. Two aliquots (10 μL) of the reaction mixture were withdrawn at each time point and spotted onto P81 phosphocellulose paper (Whatman) in the case of peptide substrates, or mixed with SDS-PAGE buffer for casein. The P81 phosphocellulose papers were washed five times with 75 mM orthophosphate and once with 100% EtOH, then placed in scintillation vials with scintillation mixture (AQUASOL-2; PerkinElmer). The incorporation of P_i was quantified using a scintillation counter (LSC-6100; Aloka) or by autoradiography after SDS-PAGE (BAS-2500; Fuji Photo Film).

Analysis of the Degradation Rate of mPER2 Protein in 293T, NIH 3T3, or *mPer2^{Luc}* MEF Cells. The intensity of the LUC::mPER2 from 293T cells, mPER2::LUC from NIH 3T3 cells, or *mPer2^{Luc}* MEFs was normalized so that the average luminescence detected at t = 0 was defined as '100'. To calculate the half-life of LUC-fused protein, the normalized results were fitted with the equation,

$$y = ae^{-kt} + (100 - a)$$

y, normalized bioluminescence intensity; *t*, time after addition of cycloheximide (CHX); *a, k*, variables. *e*, Napier's constant.

And the half-life $t_{1/2}$ was calculated as follows:

$$t_{1/2} = -\ln\left(\frac{(a - 50)}{a}\right)\frac{1}{k}.$$

Analysis of the Temperature Sensitivity of mPER2 Degradation in the *mPer2^{Luc}* MEFs. The cultures were maintained at 27 °, 32 °, or 37 °C for 4 days, and the bioluminescence from the cells was monitored by the PMT-Tron system until the oscillations of the bioluminescence from mPER2::LUC triggered by the temperature change were diminished. The cells were then treated with 400

μg/mL CHX. The bioluminescence was recorded every 30 min for 5 h by the PMT-Tron system. The time course of the bioluminescence in each well was normalized and analyzed as described for the degradation rate of the LUC::mPER2 protein in 293T cells.

Construction of Expression Vectors for a Reporter Assay to Examine Clock-Related Protein Stability. To investigate the stability of clock-related proteins (PER2, PER1, and BMAL1) in cultured 293T cells, we constructed an expression plasmid bearing the firefly Luciferase protein fused to the N-terminal end of clock-related proteins (LUC::mPER2, LUC::mPER1, and LUC::mBMAL1) under the CMV promoter (CMV-*Luc*::*mPer2*, CMV-*Luc*::*mPer1*, and CMV-*Luc*::*mBmal1*). We also constructed an expression vector bearing the firefly luciferase protein fused to the C-terminal end of the mouse Per2 protein (mPER2::LUC) using a custom expression vector pMU2 (18) for studies in cultured NIH 3T3 cells (pMU2-*mPer2*::*Luc*). The cDNAs of these clock-related proteins were kindly provided by Dr. H. Tei (Mitsubisi Kagaku Institute for Life Sciences, Japan). A control expression vector expressing the LUC protein under the CMV promoter (CMV-*Luc*) was also constructed.

The coding sequence of *mCKIε*(wt) was subcloned into the pMU2 expression vector as previously described [pMU2-*mCKIε*(wt)]. An expression vector for the *mCKIε*(*tau*) mutant (in which Arg-178 was replaced with Cys) was constructed by inverse PCR using pMU2-*mCKIε*(wt) as a template. Inverse PCR was performed using the following PCR primers.

F: 5′-TGCTATGCCTCTATCAACACCCAC-3′

R: 5′-GGCAGTGCCGGTCAGGTTCTTG-3′ (the 5′ end was phosphorylated).

Finally, self-ligation of the PCR product was performed. The resultant vector was named pMU2-*mCKIε*(*tau*).

An expression vector bearing only the catalytic domain of mCKIε (ΔmCKIε) was also constructed. The coding sequence of the regulatory domain of mCKIε, corresponding to amino acids 320 to 416, was deleted from pMU2-*mCKIε*(wt) by inverse PCR. The resultant vector was named pMU2-Δ*mCKIε*(wt).

The *mCKIε*(wt), *mCKIε*(*tau*), or Δ*mCKIε*(wt) gene was fused in-frame with 1× *Flag* Tag at the N terminus, and regulated by the CMV promoter.

Analysis of mPER2 Protein Stability in 293T Cells. 293T cells transfected with expression vectors for LUC::mPER2, CKIε(*tau*), and *Renilla* Luciferase were subcultured on 96- or 384-well culture plates. The stability of the LUC::mPER2 protein was measured after a 24-h incubation with a chemical compound, and the degradation rate of LUC::mPER2 was determined at the indicated times after adding 200 μg/mL CHX. The LUC activity was measured using the Dual-Glo bioluminescence detection kit (Promega) following the manufacturer's protocol. The degradation rate was calculated as described above.

Western Blot of mPER2 Protein Expressed in 293T Cells. 293T cells, grown in DMEM supplemented with 10% FBS and antibiotics (25 U/mL penicillin, 25 mg/mL streptomycin; Invitrogen), were plated at 4×10^5 cells per dish in 35-mm dishes. Twenty-four hours later, the cells were transfected with FuGene6 (Roche), according to the manufacturer's instructions. The cells were transfected with 2 μg pcDNA3-*Myc-mPer2* (a gift from Dr. E. Nishida, Kyoto University) (23), 2 μg pMU2-*mCKIε*(*tau*), or empty plasmid pMU2, and 2 μg pMU2-*Luc*. After 24 h, the cells transfected with the *mCKIε*(*tau*) expression vector were harvested, combined, and then replated onto the same number of 35-mm dishes to normalize for variations in the transfection efficiencies due to different plates. After 48 h, the cells were treated with or without 100 μM TG003 or SP600125 in 0.2% DMSO (Nacalai Tesque). The treated cells were harvested at the times indicated in Fig. S4, lysed with the extraction reagent [50 mM Tris-HCl, pH 8.1, 10 mM EDTA, 1% SDS, Halt Protease Inhibitor Mixture, EDTA-free (Pierce)], and sonicated. The protein concentration of the samples was measured by the Bradford method using a Bio-Rad Laboratories protein assay kit (Bio-Rad Laboratories). Equal amounts of protein (0.25 mg) were then mixed with NuPAGE LDS sample buffer (Invitrogen), and the samples were separated by electrophoresis and transferred to PVDF membranes using the NuPAGE electrophoresis system (Invitrogen), as described in the manufacturer's protocol. Myc-mPER2 protein was detected with an anti-Myc monoclonal antibody (clone A-14; Santa Cruz Biotechnology.) and HRP-conjugated anti-rabbit IgG secondary antibody (GE Healthcare). An anti-tubulinα monoclonal antibody (clone DM1A; LAB VISION) and anti-mouse IgG secondary antibody (GE Healthcare) were used to detect tubulinα protein. The immunoreactivities were visualized and quantified using the ECL Plus Western Blotting Detection system (GE Healthcare) and LAS-1000 (Fujifilm), according to the manufacturers' instructions.

Analysis of Temperature Sensitivity of mPER2 or LUC Degradation in NIH 3T3 Cells. NIH 3T3 cells cultured on 100-mm plates were transfected with 30 μg reporter vector (pMU2-*mPer2*::*Luc* or pMU2-*Luc*) and 6 μg pMU2-Δ*CKIε*(wt) or empty pMU2 using 60 μL FuGene6. The transfected cells were dissociated by trypsin and plated on 24-well culture plates 24 h after transfection, and the degradation of mPER2::LUC or LUC was measured as described above for $mPer2^{Luc}$ MEFs.

1. Hirota T, et al. (2008) A chemical biology approach reveals period shortening of the mammalian circadian clock by specific inhibition of GSK-3beta. *Proc Natl Acad Sci USA* 105:20746–20751.
2. Liu AC, Lewis WG, Kay SA (2007) Mammalian circadian signaling networks and therapeutic targets. *Nat Chem Biol* 3:630–639.
3. Eide EJ, et al. (2005) Control of mammalian circadian rhythm by CKIepsilon-regulated proteasome-mediated PER2 degradation. *Mol Cell Biol* 25:2795–2807.
4. O'Neill JS, et al. (2008) cAMP-dependent signaling as a core component of the mammalian circadian pacemaker. *Science* 320:949–953.
5. Vanselow K, et al. (2006) Differential effects of PER2 phosphorylation: Molecular basis for the human familial advanced sleep phase syndrome (FASPS). *Genes Dev* 20:2660–2672.
6. Abe M, Herzog ED, Block GD (2000) Lithium lengthens the circadian period of individual suprachiasmatic nucleus neurons. *Neuroreport* 11:3261–3264.
7. Iwahana E, et al. (2004) Effect of lithium on the circadian rhythms of locomotor activity and glycogen synthase kinase-3 protein expression in the mouse suprachiasmatic nuclei. *Eur J Neurosci* 19:2281–2287.
8. Chansard M, et al. (2007) c-Jun N-terminal kinase inhibitor SP600125 modulates the period of mammalian circadian rhythms. *Neuroscience* 145:812–823.
9. Hayashi Y, et al. (2003) p38 mitogen-activated protein kinase regulates oscillation of chick pineal circadian clock. *J Biol Chem* 278:25166–25171.
10. Jainchill JL, Aaronson SA, Todaro GJ (1969) Murine sarcoma and leukemia viruses: assay using clonal lines of contact-inhibited mouse cells. *J Virol* 4:549–553.
11. Ponten J, Saksela E (1967) Two established in vitro cell lines from human mesenchymal tumours. *Int J Cancer* 2:434–447.
12. Meis PJ (2005) 17 Hydroxyprogesterone for the prevention of preterm delivery. *Obstet Gynecol* 105:1128–1135.
13. Wang RH, Tao L, Trumbore MW, Berger SL (1997) Turnover of the acyl phosphates of human and murine prothymosin alpha in vivo. *J Biol Chem* 272:26405–26412.
14. Sippel CJ, Dawson PA, Shen T, Perlmutter DH (1997) Reconstitution of bile acid transport in a heterologous cell by cotransfection of transporters for bile acid uptake and efflux. *J Biol Chem* 272:18290–18297.
15. Kennedy HJ, et al. (1999) Glucose generates sub-plasma membrane ATP microdomains in single islet beta-cells. Potential role for strategically located mitochondria. *J Biol Chem* 274:13281–13291.
16. Flotow H, et al. (1990) Phosphate groups as substrate determinants for casein kinase I action. *J Biol Chem* 265:14264–14269.
17. Xu Y, et al. (2007) Modeling of a human circadian mutation yields insights into clock regulation by PER2. *Cell* 128:59–70.
18. Ukai H, et al. (2007) Melanopsin-dependent photo-perturbation reveals desynchronization underlying the singularity of mammalian circadian clocks. *Nat Cell Biol* 9:1327–1334.
19. Sato TK, et al. (2006) Feedback repression is required for mammalian circadian clock function. *Nat Genet* 38:312–319.
20. Yoo SH, et al. (2004) PERIOD2::LUCIFERASE real-time reporting of circadian dynamics reveals persistent circadian oscillations in mouse peripheral tissues. *Proc Natl Acad Sci USA* 101:5339–5346.

21. Gietzen KF, Virshup DM (1999) Identification of inhibitory autophosphorylation sites in casein kinase I epsilon. *J Biol Chem* 274:32063–32070.
22. Lowrey PL, et al. (2000) Positional syntenic cloning and functional characterization of the mammalian circadian mutation tau. *Science* 288:483–492.
23. Akashi M, Tsuchiya Y, Yoshino T, Nishida E (2002) Control of intracellular dynamics of mammalian period proteins by casein kinase I epsilon (CKIepsilon) and CKIdelta in cultured cells. *Mol Cell Biol* 22:1693–1703.
24. Meijer L, et al. (1997) Biochemical and cellular effects of roscovitine, a potent and selective inhibitor of the cyclin-dependent kinases cdc2, cdk2 and cdk5. *Eur J Biochem* 243:527–536.
25. Muraki M, et al. (2004) Manipulation of alternative splicing by a newly developed inhibitor of Clks. *J Biol Chem* 279:24246–24254.
26. Bain J, et al. (2007) The selectivity of protein kinase inhibitors: A further update. *Biochem J* 408:297–315.
27. Kummer JL, Rao PK, Heidenreich KA (1997) Apoptosis induced by withdrawal of trophic factors is mediated by p38 mitogen-activated protein kinase. *J Biol Chem* 272:20490–20494.
28. Fong TA, et al. (1999) SU5416 is a potent and selective inhibitor of the vascular endothelial growth factor receptor (Flk-1/KDR) that inhibits tyrosine kinase catalysis, tumor vascularization, and growth of multiple tumor types. *Cancer Res* 59:99–106.
29. Zandomeni R, Weinmann R (1984) Inhibitory effect of 5,6-dichloro-1-beta-D-ribofuranosylbenzimidazole on a protein kinase. *J Biol Chem* 259:14804–14811.
30. Ghai G, et al. (1987) Pharmacological characterization of CGS 15943A: A novel nonxanthine adenosine antagonist. *J Pharmacol Exp Ther* 242:784–790.
31. Kim YC, Ji XD, Jacobson KA (1996) Derivatives of the triazoloquinazoline adenosine antagonist (CGS15943) are selective for the human A3 receptor subtype. *J Med Chem* 39:4142–4148.
32. Kraichely DM, Sun J, Katzenellenbogen JA, Katzenellenbogen BS (2000) Conformational changes and coactivator recruitment by novel ligands for estrogen receptor-alpha and estrogen receptor-beta: Correlations with biological character and distinct differences among SRC coactivator family members. *Endocrinology* 141:3534–3545.
33. Ashley RL, et al. (2006) Cloning and characterization of an ovine intracellular seven transmembrane receptor for progesterone that mediates calcium mobilization. *Endocrinology* 147:4151–4159.
34. Baker ME, et al. (1984) Chick oviduct progesterone receptor binding of 15 beta, 17-dihydroxyprogesterone and its analogues. *Steroids* 43:153–158.
35. Nelson EM, Tewey KM, Liu LF (1984) Mechanism of antitumor drug action: Poisoning of mammalian DNA topoisomerase II on DNA by 4′-(9-acridinylamino)-methanesulfon-m-anisidide. *Proc Natl Acad Sci USA* 81:1361–1365.
36. Eagling VA, Tjia JF, Back DJ (1998) Differential selectivity of cytochrome P450 inhibitors against probe substrates in human and rat liver microsomes. *Br J Clin Pharmacol* 45:107–114.
37. Yoon KW, Covey DF, Rothman SM (1993) Multiple mechanisms of picrotoxin block of GABA-induced currents in rat hippocampal neurons. *J Physiol* 464:423–439.
38. Smith DG, et al. (2001) 3-Anilino-4-arylmaleimides: Potent and selective inhibitors of glycogen synthase kinase-3 (GSK-3). *Bioorg Med Chem Lett* 11:635–639.
39. Pilla M, et al. (1999) Selective inhibition of cocaine-seeking behaviour by a partial dopamine D3 receptor agonist. *Nature* 400:371–375.
40. Johnson RA, et al. (1997) Isozyme-dependent sensitivity of adenylyl cyclases to P-site-mediated inhibition by adenine nucleosides and nucleoside 3′-polyphosphates. *J Biol Chem* 272:8962–8966.
41. Thompson RD, Secunda S, Daly JW, Olsson RA (1991) Activity of N6-substituted 2-chloroadenosines at A1 and A2 adenosine receptors. *J Med Chem* 34:3388–3390.
42. Kemppainen JA, et al. (1999) Distinguishing androgen receptor agonists and antagonists: Distinct mechanisms of activation by medroxyprogesterone acetate and dihydrotestosterone. *Mol Endocrinol* 13:440–454.
43. Jacobson KA, et al. (1995) Structure-activity relationships of 9-alkyladenine and ribose-modified adenosine derivatives at rat A3 adenosine receptors. *J Med Chem* 38:1720–1735.
44. Meyers MJ, et al. (2001) Estrogen receptor-beta potency-selective ligands: Structure-activity relationship studies of diarylpropionitriles and their acetylene and polar analogues. *J Med Chem* 44:4230–4251.
45. Nymark M, et al. (1973) Prolonged neuroleptic effect of alpha-flupenthixol decanoate in oil. *Acta Pharmacol Toxicol (Copenh)* 33:363–376.
46. Faust R, et al. (2000) Mapping the melatonin receptor. 6. Melatonin agonists and antagonists derived from 6H-isoindolo[2,1-a]indoles, 5,6-dihydroindolo[2,1-a]isoquinolines, and 6,7-dihydro-5H-benzo[c]azepino[2,1-a]indoles. *J Med Chem* 43:1050–1061.
47. Garvin JL, Simon SA, Cragoe EJ, Jr, Mandel LJ (1985) Phenamil: An irreversible inhibitor of sodium channels in the toad urinary bladder. *J Membr Biol* 87:45–54.
48. Kennett GA, et al. (1996) In vitro and in vivo profile of SB 206553, a potent 5-HT2C/5-HT2B receptor antagonist with anxiolytic-like properties. *Br J Pharmacol* 117:427–434.
49. Lal B, et al. (1984) Trequinsin, a potent new antihypertensive vasodilator in the series of 2-(arylimino)-3-alkyl-9,10-dimethoxy-3,4,6,7-tetrahydro-2H-py rim ido [6,1-a]isoquinolin-4-ones. *J Med Chem* 27:1470–1480.
50. Knauf U, Tschopp C, Gram H (2001) Negative regulation of protein translation by mitogen-activated protein kinase-interacting kinases 1 and 2. *Mol Cell Biol* 21:5500–5511.
51. Showalter VM, Compton DR, Martin BR, Abood ME (1996) Evaluation of binding in a transfected cell line expressing a peripheral cannabinoid receptor (CB2): Identification of cannabinoid receptor subtype selective ligands. *J Pharmacol Exp Ther* 278:989–999.

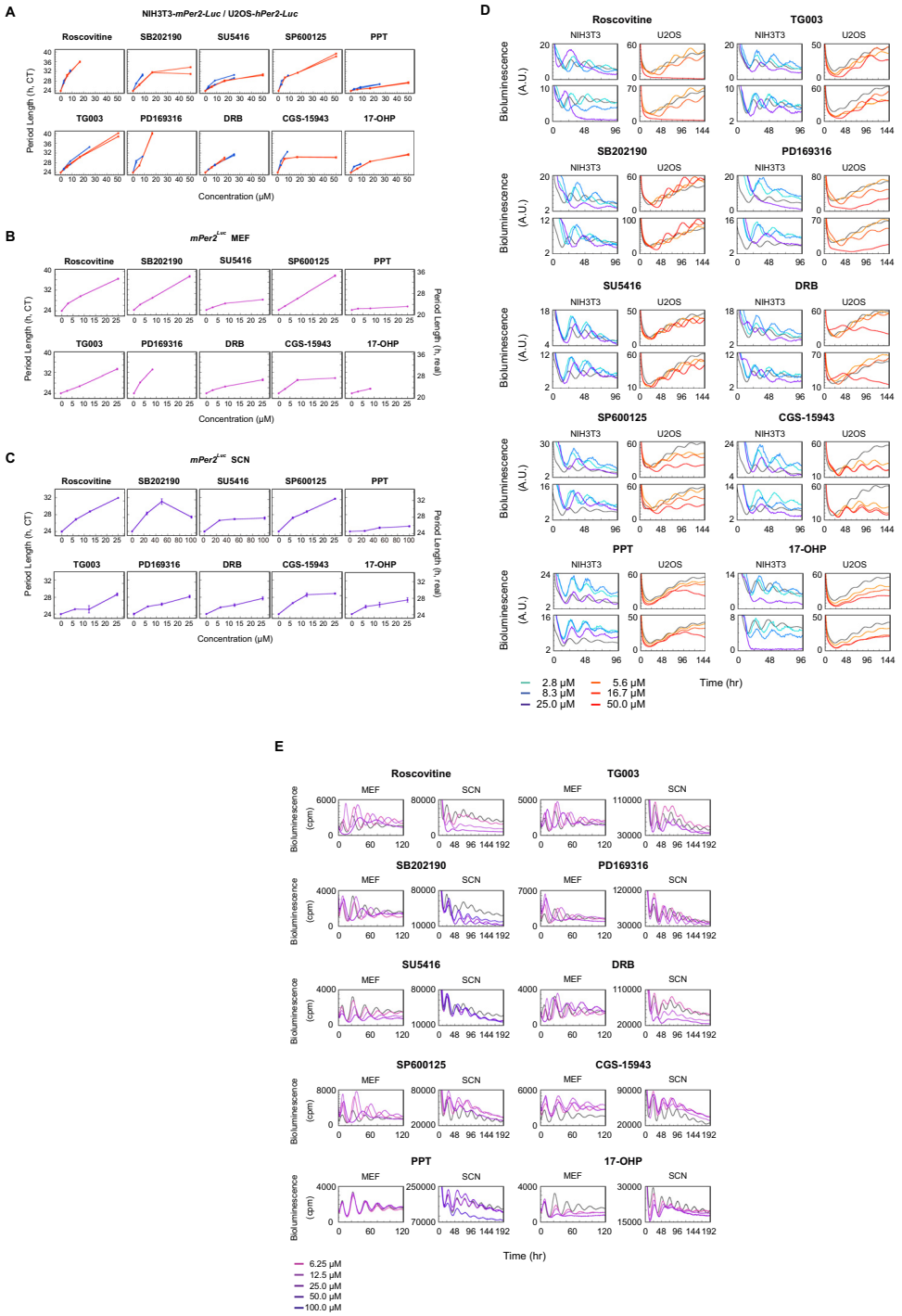

Fig. S1. Dose-response of period length in the NIH 3T3-*mPer2-Luc* and U2OS-*hPer2-Luc* cells (*A*), primary cultures of MEFs (*B*), slice cultures of SCN (*C*) from *mPer2*^{Luc} mice, and raw bioluminescence data (*D* and *E*). The period length were represented both in real time (right axis in *B* and *C*) and in circadian time (i.e., the period length of control samples was adjusted to 24 h, left axis). Blue circles in (*A*) represented average of NIH 3T3 ($n = 2$) and red squares U2OS ($n = 3$). Each line represented independent experiments. Each value in (*B* and *C*) represents the mean ± SEM. At the concentrations without data points, the cells behaved arrhythmically. (*D*) Time course of the reporter activity in NIH 3T3-*mPer2-Luc* cells (left panels) and U2OS-*hPer2-Luc* cells (right panels) after forskolin stimulation and the addition of compound. The gray lines represent the average of control samples ($n = 768$ for NIH 3T3, and $n = 96$ for U2OS) and colored lines represent the averages of samples containing compounds at the concentrations indicated at the base of the figure ($n = 2$ for NIH 3T3, and $n = 3$ for U2OS). The compound name is displayed at the top of each set of four panels. The upper and lower panels within each group indicate separate experiments. (*E*) Time course of the reporter activity in MEFs (left panels) and SCN slices (right panels) after stimulation with compound with (MEFs) or without (SCN) forskolin. The gray lines represent the average of control samples ($n = 5$ for MEF, and $n = 4$ for SCN) and colored lines represent the average of samples containing compound at the concentrations indicated at the bottom of the figure ($n = 3$ for MEF, and $n = 4$ for SCN). The compound represented in the graphs is written above each pair of panels.

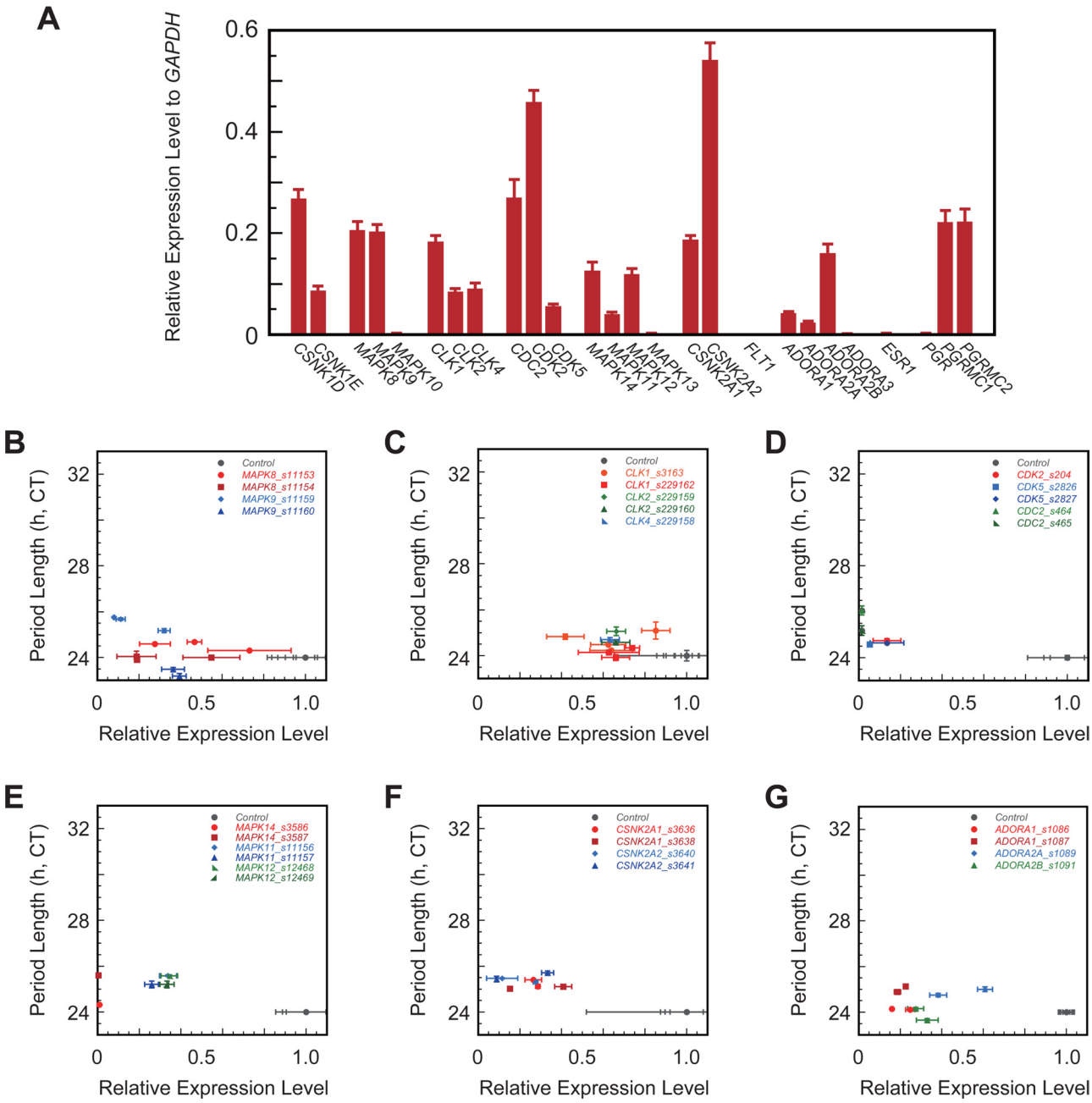

Fig. S2. Effects of gene knockdowns on the period length in U2OS-*hPer2-Luc cells*. (*A*) Relative expression levels of CKIε, CKIδ and genes related to the 10 potent chemical compounds that lengthened the period length (see Table S3), examined by the quantitative real-time PCR method. The graph indicates the average + SEM of the gene expressions relative to *GAPDH* ($n = 6$). The expression of the *FLT1* gene was undetectable. (*B–G*) Relationship between gene knockdown effects and period length in U2OS-*hPer2-Luc* cells. Two sets of U2OS-*hPer2-Luc* cells were transfected with predesigned *Silencer* Select siRNA: One was cultured on the PMT-Tron system for measurement of the period length, and the other was analyzed for gene expression levels 24 h after the transfection. The x-axis indicates the expression level of genes relative to the samples transfected with control siRNA. The y-axis indicates the period length, described in circadian time (CT), with the control samples assigned as 24 h. Each symbol represents the mean ± SEM. of independent experiments ($n \geq 3$). (*B*) Gene knockdowns of kinases inhibited by SP600125. *MAPK8*, mitogen-activated protein kinase 8 [MAPK8, also c-Jun N-terminal kinase 1 (JNK1)]; *MAPK9*, MAPK9 (JNK2). (*C*) Gene knockdowns of kinases inhibited by TG003. *CLK1*, CDC-like kinase 1 (CLK1); *CLK2*, CLK2; *CLK4*, CLK4. (*D*) Gene knockdowns of kinases inhibited by Roscovitine. *CDK1*, Cyclin-dependent kinase 1 (CDK1); *CDK2*, CDK2; *CDK4*, CDK4. (*E*) Gene knockdowns of kinases inhibited by SB202190 and PD169316. *MAPK14*, MAPK14 [also p38 MAPK α (p38α)]; *MAPK11*, MAPK11 (p38β); *MAPK12*, MAPK12 (p38γ). (*F*) Gene knockdowns of kinases inhibited by DRB. *CSNK2A1*, CK2α; *CSNK2A2*, CK2α′. (*G*) Gene knockdowns of adenosine receptors inhibited by CGS-15943. *ADORA1*, Adenosine A1 receptor; *ADORA2A*, Adenosine A2a receptor; *ADORA2B*, Adenosine A2b receptor

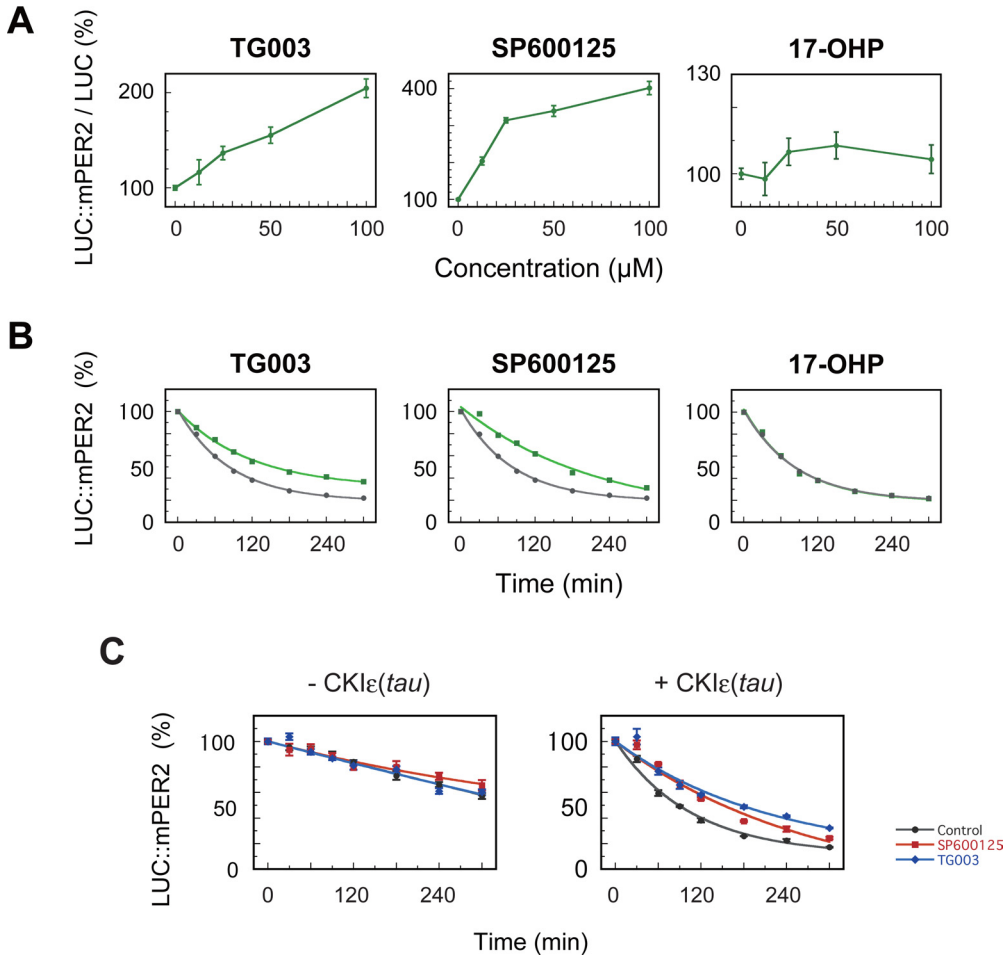

Fig. S3. Effect of the potent effective compounds on the stability of mPER2 proteins in cellulo. (*A*) mPER2 stabilization in 293T cells. Bioluminescence from 293T cells cotransfected with a reporter (LUC::mPER2 or LUC) and CKIε(*tau*) was measured, and the ratio of the bioluminescence of LUC::mPER2 to LUC was plotted. Each value represents the mean ± SEM. ($n = 16$ for 0 μM, $n = 4$ for chemically treated samples). All of the compounds except 17-OHP exhibited a significant dose-dependent effect ($P < 0.01$; one-way ANOVA). (*B*) mPER2 degradation rate in 293T cells. The averages ($n = 3$; closed circles) of the normalized bioluminescence of 293T cells cotransfected with the LUC::mPER2 reporter and CKIε(*tau*) after treatment with CHX in the presence (green) or absence (gray) of a chemical compound were plotted. The fitted curve is also indicated in each panel. The time course of all of the samples except 17-OHP was significantly different from that of the control samples ($P < 0.001$; two-way ANOVA). (*C*) The potent inhibitors dominantly affected the CKI-dependent degradation of LUC::mPER2 but not the CKI-independent degradation. The average ± SEM. ($n = 3$) of the normalized bioluminescent activities of 293T cells cotransfected with the LUC::mPER2 reporter and CKIε(*tau*) (right panel) or control vector (left panel) with 100 μM SP600125 (red squares), TG003 (blue diamonds), or solvent only (0.25% DMSO; gray circles) after treatment with CHX was plotted. The fitted curve is also indicated in each panel.

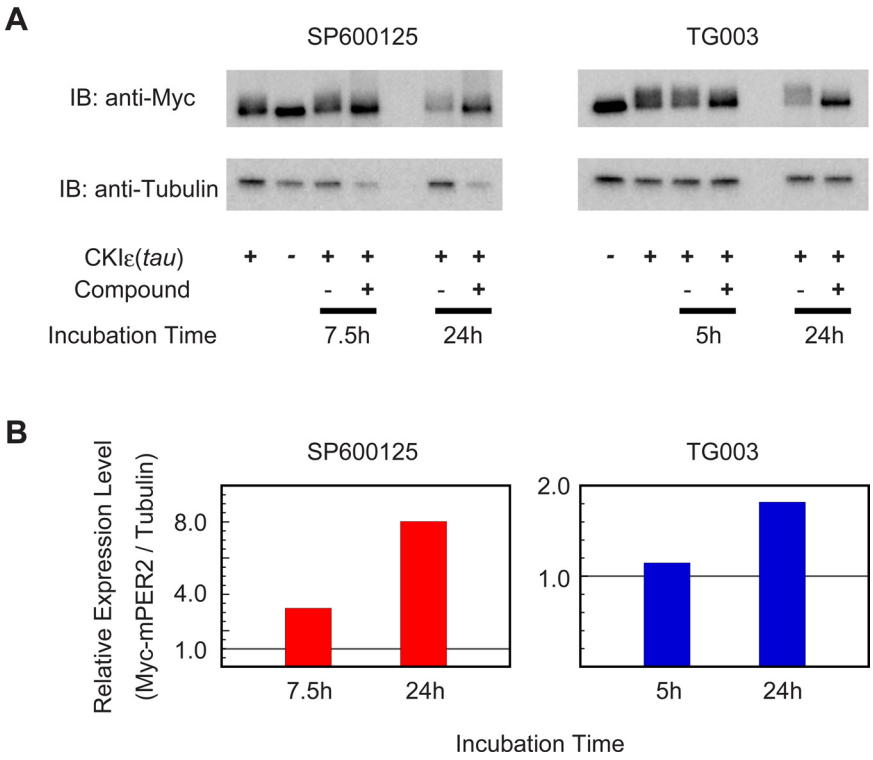

Fig. S4. Effects of SP600125 and TG003 on mPER2 stabilization in 293T cells. (*A*) 293T cells cotransfected with Myc-tagged mPER2 (Myc-mPER2) and CKIε(*tau*) were incubated with or without 100 μM SP600125 (*Left*) or TG003 (*Right*) for the indicated times, and the lysates were collected and analyzed by Western blotting. Equal portions of three samples were mixed and analyzed in each lane. Myc-mPER2 was detected with an anti-Myc antibody (upper panels) and Tubulin was also blotted as an internal control (lower panels). Note that the two compounds inhibited the mobility shift of mPER2 caused by the coexpression with CKIε(*tau*). (*B*) Quantification of the results of (*A*). The densities of immunoreactive bands were measured, and the density of Myc-mPER2 was normalized to that of Tubulin in the same sample (Myc-mPER2/tubulin). The graph represents the relative value of Myc-mPER2/Tubulin at the indicated incubation times with 100 μM SP600125 (*Left*) or TG003 (*Right*) compared with the control (DMSO) samples.

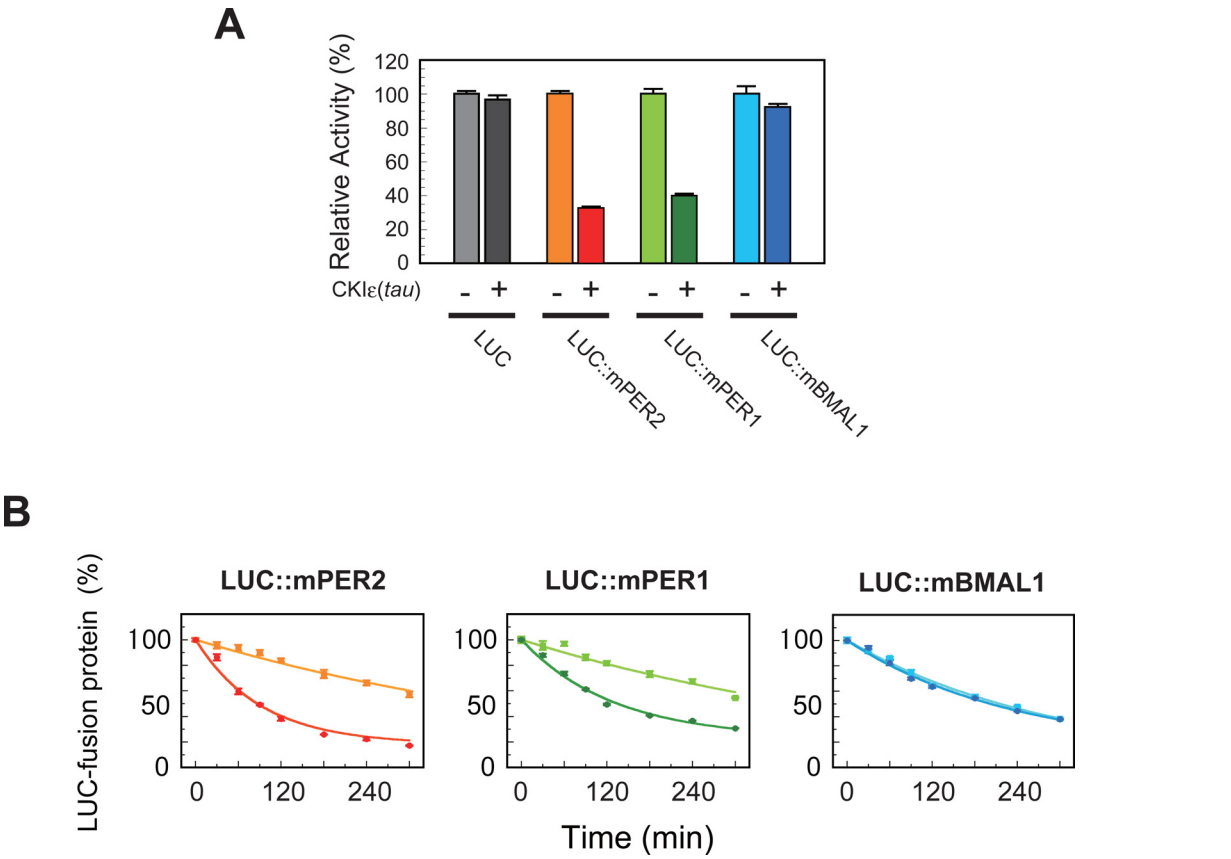

Fig. S5. CKIε(*tau*) destabilizes the LUC::mPER2 and LUC::mPER1 proteins but not LUC or LUC::mBMAL1. (*A*) Effects of CKIε(*tau*) on the stability of Luciferase-fused clock proteins in 293T cells. The Luciferase activity in 293T cells transfected with the expression vector for LUC, LUC::mPER2, LUC::mPER1, or LUC::mBMAL1, and CKIε(*tau*) was measured 48 h after transfection. Note that the co-expression with CKIε(*tau*) attenuated the bioluminescent activity of LUC::mPER2 and LUC::mPER1, but not of LUC or LUC::mBMAL1. Each value represents the mean + SEM ($n = 4$). (*B*) Effects of CKIε(*tau*) on the degradation rates of Luciferase-fused clock proteins in 293T cells. The average ± SEM. ($n = 3$) of the normalized bioluminescent activities of 293T cells cotransfected with LUC-fused clock protein reporters (LUC::mPER2, LUC::mPER1, or LUC::mBMAL1) and CKIε(*tau*) (circles) or control vector (squares) after treatment with CHX was plotted. The fitted curve is also indicated in each panel.

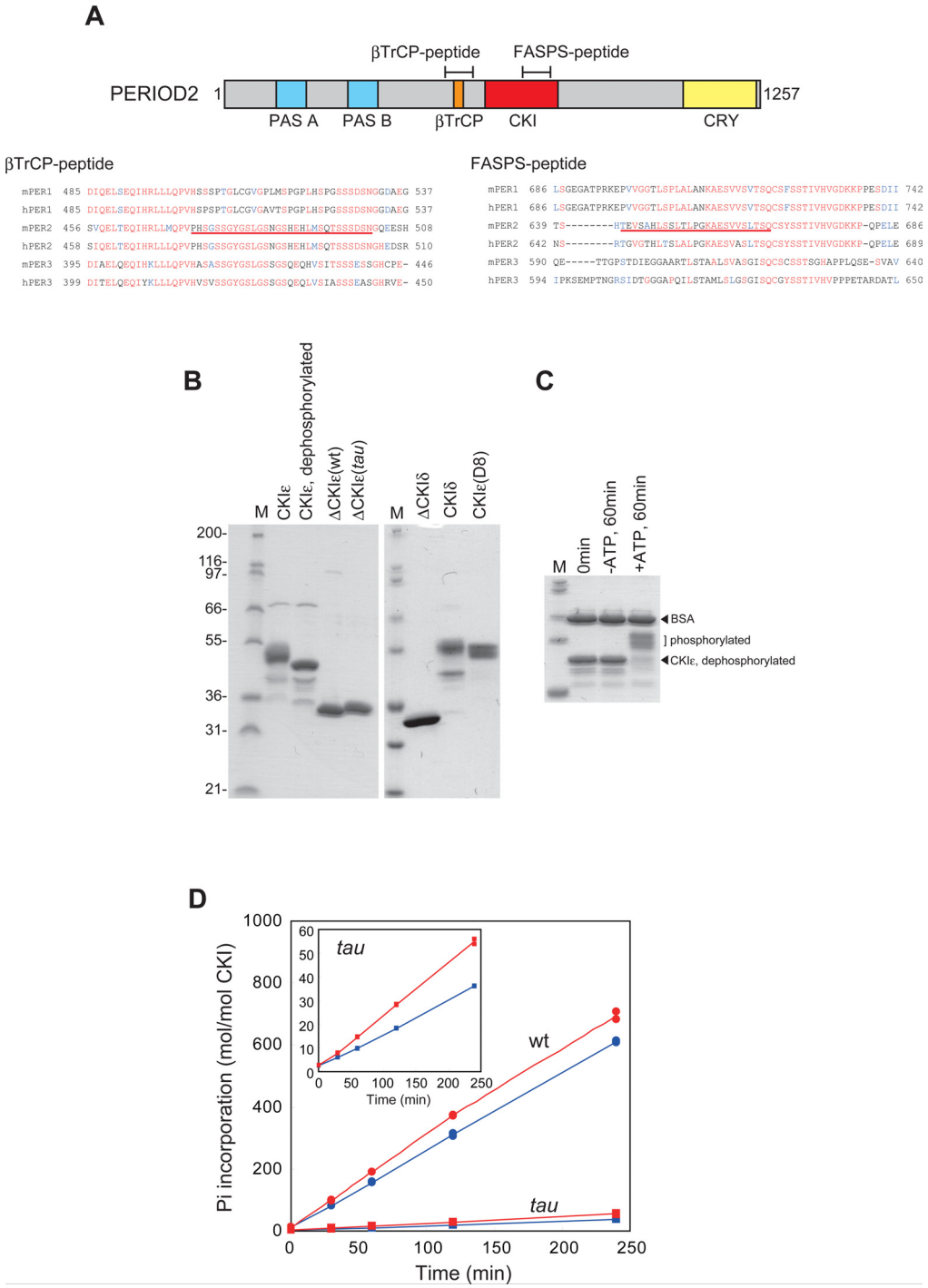

Fig. S6. Temperature insensitivity of the CKIε phosphorylation activity. (*A*) Schematic diagram of PERIOD2 (PER2) and the sequence alignment around the βTrCP-binding (SSGYGS) and FASPS motif. Locations of the PAS domains (light blue), the βTrCP-binding motif (orange), the CKI-binding domain (red), and the CRYPTOCHROME-binding domain (yellow) are indicated. Location corresponding to the amino acid sequence of the synthetic peptide substrate is indicated by bars above the diagram. Sequence corresponding to the βTrCP-peptide (amino acids 473–502, a serine-rich region around the βTrCP-binding motif in PER2) and FASPS-peptide (amino acids 642–666, a region around FASPS-related phosphorylation sites) are underlined in the aligned sequence. (*B*) The catalytic domains of CKIε (wt) and CKIε (tau) [ΔCKIε(*tau*) and ΔCKIε(wt)] and full-length CKIε were purified as described in the Materials and Methods, separated by electrophoresis, and stained with Coomassie Brilliant Blue. (*C*) Autophosphorylation of CKIε before performing in vitro kinase assays. Dephosphorylated CKIε was incubated with or without ATP for 60 min. Note that CKIε was phosphorylated by the incubation with ATP (right-most lane). Lanes ''M'' in both (*B*) and (*C*) were standard molecular weight markers. (*D*) Phosphorylation of FASPS-peptide by ΔCKIε(wt) (circles) and ΔCKIε(*tau*) (squares) was assayed at 25 °C (blue) and 35 °C (red). (Inset) Expanded plot of the ΔCKIε(*tau*) phosphorylation activity. Assay conditions are described in the experimental procedures.

Other Supporting Information Files

Table S1
Table S2
Table S3
Table S4